Received: 10 February 2020 | Revised: 26 March 2020 | Accepted: 6 April 2020

DOI: 10.1002/aoc.5762

Applied Organometallic Chemistry WILEY

FULL PAPER

An insight into the potent antioxidant activity of a dithiocarbohydrazone appended *cis*-dioxidomolybdenum (VI) complexes

T.M. Asha[1] | **M.R. Prathapachandra Kurup**[1,2]

[1]Department of Applied Chemistry, Cochin University of Science and Technology, Kochi, Kerala, 682 022, India

[2]Department of Chemistry, School of Physical Sciences, Central University of Kerala, Tejaswini Hills, Periye, Kasargode, Kerala, 671 320, India

Correspondence
M. R. Prathapachandra Kurup, Department of Applied Chemistry, Cochin University of Science and Technology, Kochi 682 022, Kerala, India.
Email: mrpcusat@gmail.com; mrp@cukerala.ac.in

In search of antioxidants with enriched potency, the present study focus on the design and synthesis of a dithiocarbohydrazone, H_3TCL derived from thiocarbohydrazide and 3-ethoxysalicylaldehyde and its coordination complexes with molybdenum, *viz*, $[MoO_2(HTCL)D]$ (**1**–**2**) (where D = methanol (**1**), DMSO (**2**)) and $[MoO_2(HTCL)D]\cdot DMF$ (where D = H_2O (**3**)). The synthesized compounds were characterised by elemental analysis, spectroscopic techniques (FT-IR, UV–vis and ^{1}H-NMR), conductivity measurements and cyclic voltammetry. Moreover the solid state structures of all the three complexes were established by single crystal X-ray diffraction analysis as mononuclear neutral species in which the molybdenum centre assumes a distorted octahedral geometry. The dithiocarbohydrazone binds to the molybdenum centre through its phenolate oxygen, O(1), azomethine nitrogen, N(1) and thioenolate sulfur, S(1) in a dianionic tridentate mode. The assessment of intermolecular contacts in the crystal arrangement was quantified using Hirshfeld surface analysis. Further the antioxidant potential of the dithiocarbohydrazone, H_3TCL and its molybdenum complexes **1**–**3** were evaluated using 1,1-diphenyl-2-picrylhydrazyl(DPPH), 2,2′-azinobis-3-ethylbenzothiazoline-6-sulfonic acid (ABTS) and total antioxidant assays. The antioxidant activities were then compared with standard antioxidant, *L*-ascorbic acid. The antioxidant potential of the synthesized compounds were then validated by molecular docking studies. Molecular modelling study was achieved to evaluate the recognition of target compound at the binding pocket of the human antioxidant enzyme, 3MNG. The docking results showed that the complexes selectively bond to the vital amino acids present in the binding pocket of the target enzyme, 3MNG.

KEYWORDS

antioxidant assay-, dithiocarbohydrazone; Hirshfeld surface analysis, *L* -ascorbic acid, molecular docking, X-ray diffraction analysis

1 | INTRODUCTION

Thiocarbohydrazones are an elite class of Schiff bases that are formed by the condensation reaction of thiocarbohydrazide with aldehydes or ketones. Since both the hydrazine groups of the thiocarbohydrazide are very reactive, they serve as favourable units for the synthesis of polyfunctional organic compounds, mostly bis-derivatives with the carbonyl compounds.[1] They are extensively used in medicinal and pharmaceutical fields owing to their ability to exhibit biological activities like antibacterial, antifungal, anticancer[2] *etc.* Due to the availability of several potential donor sites, they find application in the self-assemblage of tetranuclear molecular square structures, in precise, mixed valence iron(II)/(III), Zn (II), Cd (II) and Ni (II) clusters.[3]

Molybdenum is the only second row transition metal that exist in a varied range of metalloenzymes and parades biological importance in various living organisms including fungi, bacteria and algae.[4] Due to the ability of molybdenum to chelate with O, N and S donor ligands, a number of molybdenum complexes with various ONO and ONS donor organic ligands have been synthesized.[5–7] Moreover the biological activities of such complexes were also been investigated. For example, molybdenum complexes derived from ONO donor aroylhydrazones were studied for their *in-vitro* cytotoxicity and antibacterial activities.[6] Similarly molybdenum complexes of an ONS donor thiosemicarbazone were demonstrated to act as models for active site of oxo-transfer molybdoenzymes.[7]

Antioxidants act as important neutraceuticals in view of their various health benefits and find application in food chemistry[8] due to their diverse roles in reducing toxic effect of oxidative stress. Even though the various biological activities of molybdenum complexes of different Schiff bases have been investigated,[6,7,9,10] their antioxidant activities seem to be much less explored.[11] In view of these findings, the present study focuses on the design and synthesis of a new dithiocarbohydrazone, H_3TCL derived from thiocarbohydrazide and 3-ethoxysalicylaldehyde (Scheme 1) as well as its dioxidomolybdenum (VI) complexes, **1**–**3** and their application in free radical scavenging.

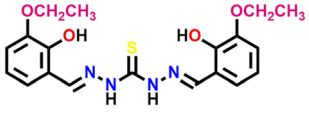

SCHEME 1 Structure of the dithiocarbohydrazone ligand, H_3TCL

2 | EXPERIMENTAL SECTION

2.1 | Materials and methods

Reagents used for the synthesis are dithiocarbohydrazine (Alfa Aesar), 3-ethoxysalicylaldehdye (Alfa Aesar) and $[MoO_2(acac)_2]$ (Sigma Aldrich). All other chemicals used were reagent grade, available commercially and used as received. Solvents were purchased from spectrochem and distilled prior to use.

Elemental analyses (CHNS) of the synthesized dithiocarbohydrazone, H_3TCL and its molybdenum complexes, **1**–**3** were executed on a Vario EL III CHNS analyzer after drying the samples. Molar conductivity measurements were performed in a 10^{-3} M solution of the molybdenum complexes in DMF at room temperature using a Systronic model 303 direct reading conductivity meter. FT-IR spectra were recorded using KBr pellets in the 4000–400 cm^{-1} range on a JASCO FT-IR 5300 spectrometer. Electronic spectra of all the synthesised compounds were recorded in UV grade DMF on Thermo Scientific Evolution 220 model UV–vis spectrophotometer in the 200–900 nm range at ambient temperature. The ^{1}H-NMR spectra were recorded in DMSO-d_6 solvent on a Bruker AMX 400 FT-NMR spectrometer at 400 MHz and tetramethylsilane (TMS) as internal standard. Redox properties of the compounds were studied on CH 6017 B instrument. The measurements were carried out using a three-electrode cell in which a Pt electrode, saturated Ag/AgCl and platinum wire are used as the working, reference and auxiliary electrodes respectively. Tetraethylammonium perchlorate (TEAP) was used as supporting electrolyte for the electrochemical work and DMSO was chosen as the solvent of analysis.

2.2 | Synthesis

2.2.1 | Synthesis of dithiocarbohydrazone, H_3TCL

The bis(3-ethoxysalicylidene)thiocarbohydrazone (H_3TCL) was prepared by the condensation reaction of thiocarbohydrazide with 3-ethoxysalicylaldehydes in a 1:2 molar ratio (Scheme 2).

To a solution of thiocarbohydrazide (0.265 g, 2.5 mmol) in methanol was added a methanolic solution of 3-ethoxysalicylaldehyde (1.610 g, 5 mmol). The resulting solution was refluxed with stirring for 3 hr in presence of few drops of glacial acetic acid. The resulting pale yellow solid thus formed was filtered off, washed with methanol and dried in air.

SCHEME 2 Synthetic pathway for the dithiocarbohydrazone, H_3TCL and its dioxidomolybdenum (VI) complexes **1–3**

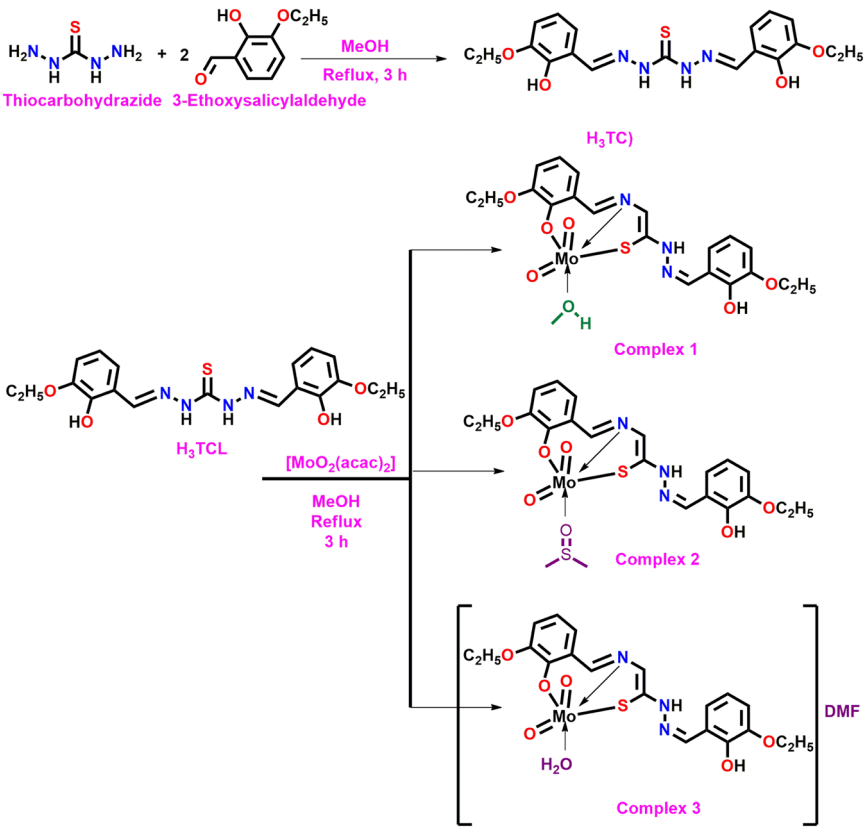

Yield: 0.3420 g, 85%. *Anal. Cal.* for $C_{19}H_{22}N_4O_4S$ (402.47 g mol^{-1}): C, 56.70; H, 5.51; N, 13.92; S, 7.97. Found: C, 56.59; H, 5.49; N, 13.97; S, 7.99. FT-IR (KBr) ν_{max}, cm^{-1}: ν(O–H) 3414, ν(N–H) 3197, ν(C=N) 1615, 1534, ν(C=S) 1370, ν(C–O) 1218. ^{1}H NMR (400 MHz, DMSO-d_6, Me_4Si, ppm) δ: 12.072, 11.875 (s, 2H, OH), 11.618, 9.142 (s, 2H, N–NH), 8.754, 8.546 (s, 2H, CH=N), 6.825–7.059 (m, 6H, aromatic), 4.065 (q, 4H, J = 6.4 Hz, OCH_2), 1.364 (t, 3H, J = 6.8 Hz CH_3). *UV/vis* (DMF) λ_{max}, nm (ε, L mol^{-1} cm^{-1}): 327 (45910), 346 (45170), 363 (39290).

2.2.2 | Synthesis of molybdenum complexes 1–3

A similar synthetic strategy was adopted for the synthesis of dioxomolybdenum(VI) complexes (Scheme 2). The reaction of $[MoO_2(acac)_2]$ with the dithiocarbohydrazone, H_3TCL in a 1:1 ratio in presence of donor solvents D (D = methanol (**1**), DMSO (**2**) and DMF (**3**)) afforded complexes **1–3**. The synthetic procedures are discussed below:

Synthesis of the molybdenum complex, [MoO_2(HTCL)(MeOH)] (1)

Methanolic solution of dithiocarbohydrazone, H_3TCL (0.402 g, 1 mmol) was mixed with a methanolic solution of the molybdenum precursor, $[MoO_2(acac)_2]$ (0.326 g, 1 mmol) and the resulting dark red coloured solution was refluxed with stirring for 5 hr. The dark red coloured product thus formed was filtered, washed with methanol and recrystallized in methanol to afford dark red block shaped crystals of complex **1**.

Yield: 0.3142 g, 56%. Molar conductance (10^{-3} M DMF): 10 Ω^{-1} cm^2 mol^{-1}. *Anal. Cal.* for $C_{20}H_{24}MoN_3O_7S$ (560.43 g mol^{-1}): C, 42.86; H, 4.32; N, 10.00; S, 5.72. Found: C, 42.81; H, 4.34; N, 10.01; S, 5.75. FT-IR (KBr) ν_{max}, cm^{-1}: ν(O–H) 3410, ν(N–H) 3196, ν(C=N) 1595, ν(C–S) 1016, ν_{sym} (*cis*-MoO_2) 936, ν_{asym} (*cis*-MoO_2) 896. ^{1}H NMR (400 MHz, DMSO-d_6, Me_4Si, ppm) δ: 11.921 (s, 1H, OH), 10.440 (s, 2H, N–NH), 8.364, 8.308 (s, 2H, CH=N), 6.811–8.284 (m, 6H, aromatic), 4.071 (q, 4H, J = 7.2 Hz, OCH_2), 1.357 (t, 3H, J = 6.8 Hz, CH_3). *UV/vis* (DMF) λ_{max}, nm (ε, L mol^{-1} cm^{-1}): 326 (36950), 348 (34470), 364 (30630), 421 (3000).

Synthesis of the molybdenum complex, [MoO_2(HTCL)(DMSO)] (2)

Methanolic solution of dithiocarbohydrazone, H_3TCL (0.402 g, 1 mmol) was added to a methanolic solution of the molybdenum precursor, $[MoO_2(acac)_2]$ (0.326 g, 1 mmol) and the resulting dark orange coloured solution was refluxed with stirring for 4 hr in presence of few drops of DMSO. The resulting dark orange coloured solution was kept aside for evaporation. The dark orange

needle shaped crystals of complex **2** thus formed after a week was separated and dried in air.

Yield: 0.3642 g, 60%. Molar conductance (10^{-3} M DMF): 7 Ω^{-1} cm^2 mol^{-1}. *Anal. Cal.* for $C_{21}H_{26}MoN_4O_7S_2$ (606.52 g mol^{-1}): C, 41.58; H, 4.32; N, 9.24; S, 10.57. Found: C, 41.53; H, 4.31; N, 9.29; S, 10.59. FT-IR (KBr) ν_{max}, cm^{-1}: ν(O–H) 3410, ν(N–H) 3189, ν(C=N) 1602, ν(C–S) 1024, ν_{sym} (*cis*-MoO_2) 929, ν_{asym} (*cis*-MoO_2) 902. ^{1}H NMR (400 MHz, DMSO-d_6, Me_4Si, ppm) δ: 11.921 (s, 1H, OH), 10.484 (s, 2H, N–NH), 8.635, 8.307 (s, 2H, CH=N), 6.811–7.826 (m, 6H, aromatic), 4.055 (q, 4H, J = 6.4 Hz, OCH_2), 1.359 (t, 3H, J = 6.8 Hz, CH_3). U*V*/*v*is (DMF) λ_{max}, nm (ε, L mol^{-1} cm^{-1}): 328 (34750), 348 (35320), 364 (32250), 421 (4620).

Synthesis of the molybdenum complex, [MoO_2(HTCL)(H_2O)]·DMF (3)

To a solution of dithiocarbohydrazone, H_3TCL (0.402 g, 1 mmol) in methanol was added the methanolic solution of the molybdenum precursor, [$MoO_2(acac)_2$] (0.326 g, 1 mmol) and the resulting dark orange coloured solution was refluxed with stirring in presence of few drops of DMF for 4 hr. The resulting dark orange coloured solution was kept aside for evaporation. The dark orange needle shaped crystals of complex **3** thus formed after a week was separated and dried in air.

Yield: 0.3410 g, 55%. Molar conductance (10^{-3} M DMF): 11 Ω^{-1} cm^2 mol^{-1}. *Anal. Cal.* for $C_{22}H_{29}MoN_5O_8S$ (619.50 g mol^{-1}): C, 42.65; H, 4.72; N, 11.30; S, 5.18. Found: C, 42.67; H, 4.76; N, 11.32; S, 5.20. FT-IR (KBr) ν_{max}, cm^{-1}: ν(O–H) 3377, ν(N–H) 3192, ν(C=N) 1595, ν(C–S) 1024, ν_{sym} (*cis*-MoO_2) 923, ν_{asym} (*cis*-MoO_2) 906. ^{1}H NMR (400 MHz, DMSO-d_6, Me_4Si, ppm) δ: 11.921 (s, 1H, OH), 10.443 (s, 2H, N–NH), 8.635, 8.307 (s, 2H, CH=N), 6.811–7.826 (m, 6H, aromatic), 4.073 (q, 4H, J = 6.8 Hz, OCH_2), 1.359 (t, 3H, J = 6.8 Hz, CH_3). U*V*/*v*is (DMF) λ_{max}, nm (ε, L mol^{-1} cm^{-1}): 328 (29880), 348 (32090), 364 (27770), 421 (2260).

2.3 | X-ray crystallography

For X-ray diffraction measurements, single crystals of the Mo complexes were mounted on a Bruker SMART APEXII CCD diffractometer, equipped with a graphite crystal, incident-beam monochromator and a fine focus sealed tube with Mo Kα (λ = 0.71073 Å) radiation as the X-ray source. The unit cell dimensions were measured and the data collection was performed. The programs SAINT and XPREP were used for data reduction and APEX2 and SAINT were used for cell refinement.[12] Absorption corrections were carried out using SADABS based on Laue symmetry using equivalent reflections.[13] The structure was solved by direct methods using SHELXS-97 and refined by full matrix least-squares refinement on F^2 using SHELXL- 2014/7 and SHELXL-2018/7[14] on a WinGX software package.[15] The anisotropic refinements were performed for all non-hydrogen atoms and all H atoms on C atoms were placed in calculated positions, guided by difference maps, with C–H bond distances of 0.93–0.96 Å. H atoms were assigned as U_{iso} = 1.2 U_{eq} (1.5 for Me). The hydrogen atoms, H(3A) and H(3′) attached to nitrogen, N(3) and O(3) respectively of all the complexes were located from difference maps and their distances were restrained using DFIX instructions with the distance restraints of N–H = 0.88 ± 0.01 Å and O–H = 0.86 ± 0.01 Å respectively. Similarly the hydrogen atoms, H(7A) and H(7B) attached to the oxygen atom O(7) of the coordinated water molecule in **3** were located from the difference map and their distances and angles were restrained using DFIX and DANG instructions with distance restraints of O–H = 0.86 ± 0.01 Å and H···H = 1.36 ± 0.02 Å, followed by refinement of their displacement parameters. Reflections, (1 0 0) and (1 1 0) of complex **1**, (0 2 1) and (0 2 0) of complex **2**; (1 1 0) and (1 0 0) of complex **3** were omitted owing to bad agreement. The molecular and crystal structures were plotted using ORTEP 3[15] and DIAMOND version 3.2 g.[16]

2.4 | Hirshfeld surface analysis

The various intermolecular interactions present in the crystal structures of the molybdenum complexes were further quantified using crystal explorer 17.5 software.[17] The Hirshfeld surface calculations were carried out with the aid of the CIF files of the crystals. The intermolecular contacts present in the crystals were mapped using normalized contact distance, d_{norm} which is defined in terms of d_i, d_e and van der Waals radii (r^{vdW}) of atoms by Equation 1.

$$\mathbf{d_{norm}} = \frac{\mathbf{d_i} - \mathbf{r_i^{vdW}}}{\mathbf{r_i^{vdW}}} + \frac{\mathbf{d_e} - \mathbf{r_e^{vdW}}}{\mathbf{r_e^{vdW}}} \quad (1)$$

Where, d_i and d_e represents the distance from the Hirshfeld surface to the nearest nucleus inside and outside the surface. This equation was visualized by employing a red-white-blue colour code. Red colour represents intermolecular contacts closer than the sum of van der Waals radii whereas the blue colour represents the regions devoid of close contacts. White colour displays the contacts around the sum of van der Waals radii. Similarly the set of points in 2D space portrays the overall

contribution of intermolecular interactions using finger print plots.[18]

2.5 | Antioxidant activity

2.5.1 | 2, 2′-Diphenyl-1-picrylhydrazyl (DPPH) radical assay

DPPH is a stable nitrogen based organic free radical[19] with a characteristic absorption band at 528 nm. It possesses a violet colour (Figure 1) in its free radical form, which changes to yellow after accepting either an electron or hydrogen radical from a compound generally regarded as an antioxidant or free radical scavenger to form the corresponding stable diamagnetic molecule. Hence DPPH assay[19] is as an easy and beneficial method for evaluating the free radical scavenging capacity of biological samples as well as organic compounds. The decrease in the absorbance of the sample at 517 nm is measured spectrophotometrically. Figure 1 represents the changes taking place during the interaction of DPPH free radical with the antioxidant compound.

The DPPH radical scavenging abilities of the dithiocarbohydrazone and its molybdenum complexes were studied by a modifying the procedure reported by Brand-Williams *et al.*[19] 1 ml of variable concentration (10–100 μM) of the compound under study in DMF was added to 1 ml methanolic solution of DPPH radical (0.5 μM) and the final volume was made to 4 ml with methanol. The solution was then incubated at 37 °C for 30 min and the decrease in the absorbance of DPPH was measured at 517 nm. The same experiment with solution devoid of thecompound under study was used as the control and the percentage inhibition of the compound was calculated using the Equation 2.

$$\%\text{Inhibition} = \frac{\mathbf{A_0} - \mathbf{A_1}}{\mathbf{A_0}} \times 100 \qquad (2)$$

Where A_0 is the absorbance of the control and A_1 is the absorbance of the sample. Then the conc. (μM) was plotted against percentage inhibition and the IC_{50} values of the dithiocarbohydrazone and its molybdenum complexes were obtained as the concentration at which the absorbance of the DPPH solution reduces to 50%. *L*-Ascorbic acid was used as the standard and all the experiments were carried out in triplicate.

2.5.2 | 2–2′- Azinobis-3-ethylbenzothiazoline-6-sulfonic acid (ABTS) assay

ABTS assay serve as a well-known method for the indirect determination of the antioxidant capacity of a compound[20] $ABTS^{\cdot+}$ is a rather stable radical that has an strong absorption around 750 nm, but in presence of peroxy radicals, it undergoes oxidation to its metastable radical form. When the ABTS radical is scavenged by an antioxidant, the absorption decreases with the disappearance of the blue/green colour of this radical (Figure 2).

The ABTS radical scavenging abilities of the dithiocarbohydrazone and its molybdenum complexes were studied by the procedure reported by Tuberoso *et al.*[21] The working solution was prepared by mixing two stock solutions of 7 mM ABTS solution and 2.4 mM potassium persulfate solution in equal amounts (1:1) and the solution was allowed to react in the dark for 12 hr at room temperature. The resulting solution was further diluted by mixing 1 ml $ABTS^{+}$ solution to obtain an absorbance of 0.706 ± 0.001 units at 734 nm using the spectrophotometer. Test samples (1 ml) were allowed to react with 1 ml of the $ABTS^{\cdot+}$ solution, followed by the absorbance reading at 734 nm after 7 min using the spectrophotometer. *L*-ascorbic acid was used as the reference standard and the control was prepared by adding the same volume of reagent without any test compound and 95% methanol. All tests and analyses were run in triplicate and the results obtained were averaged. The percentage inhibition was calculated as ABTS radical scavenging activity using Equation 2.

2.5.3 | Total antioxidant assay

Total antioxidant capacity (TAC) assay by phosphor-molybdenum method is based on the reduction of Mo (VI) by the sample analyte and subsequent formation of a green phosphate-Mo(V) complex (Figure 3) at acidic pH.

The total antioxidant capacity of the dithiocarbohydrazone and its molybdenum complexes

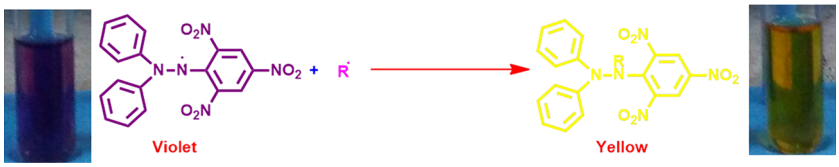

FIGURE 1 The changes taking place during the interaction of DPPH radical with the free radical scavenger

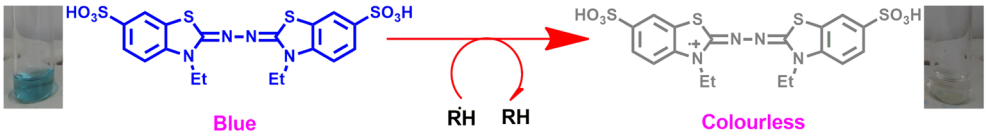

FIGURE 2 The changes taking place during the interaction of ABTS radical with the free radical scavenger

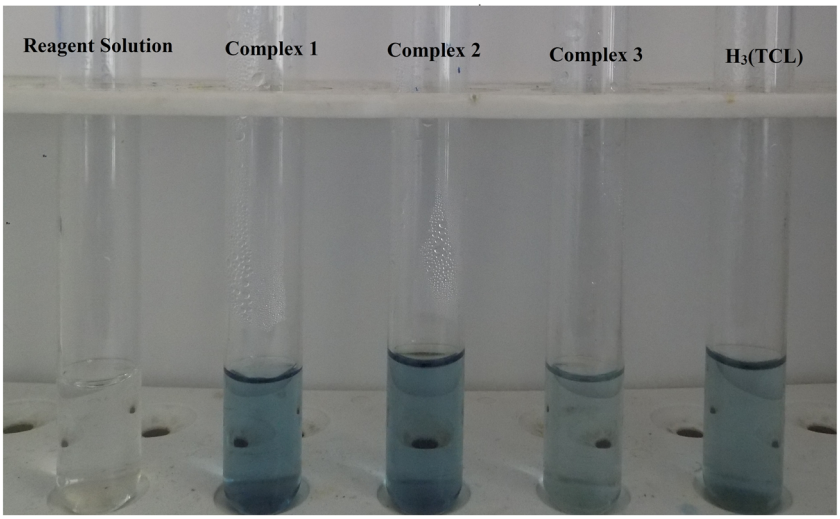

FIGURE 3 The colour change taking place during the interaction of phosphomolybdenum reagent with the free radical scavengers

were evaluated by the phosphor-molybdenum method, according to the procedure described by Prieto *et al.*[22] 100 μL of sample was combined with 3 ml of reagent solution (0.6 M sulfuric acid, 28 mM sodium phosphate and 4 mM ammonium molybdate). The tubes containing the reaction solution were incubated at 95 °C for 90 min. Then, the absorbance of the solution was measured at 695 nm using a UV–vis. Spectrophotometer against blank after cooling to room temperature. The total antioxidant activity was expressed as the number of gram equivalent of ascorbic acid. The calibration curve was prepared by mixing *L*- ascorbic acid with methanol.

3 | RESULTS AND DISCUSSION

3.1 | Synthesis and characterization

Dithiocarbohydrazone, H_3TCL and its molybdenum complexes **1**–**3** were isolated in good to excellent yields and characterized by elemental analysis as well as various physicochemical techniques. The dithiocarbohydrazone was obtained as white solid, whereas all the molybdenum complexes were obtained as dark orange crystalline solids. Both the dithiocarbohydrazone and its complexes were air stable at room temperature. They were found to be completely soluble in DMSO, DMF and acetonitrile; partially soluble in methanol and ethanol and completely insoluble in CCl_4, $CHCl_3$ and water. The ligand and the complexes portrayed excellent free radical scavenging activities.

3.2 | Spectral characterization

3.2.1 | Vibrational spectra

The FT-IR spectrum of the dithiocarbohydrazone, H_3TCL exhibits bands at 3290 and 3155 cm^{-1} corresponding to the ν(O–H) and ν(N–H) stretching vibrations respectively.[7][,3(e,2(d))] Presence of the bands (ν(O–H) = 3377–3410 cm^{-1} and ν(N–H) = 3189–3196 cm^{-1}) in the spectra of the molybdenum complexes **1**–**3** indicate that one of the OH and NH groups are still retained in each molybdenum complex without coordinating to the metal centre. Weak bands at 1609 and 1585 cm^{-1} in the spectrum of the dithiocarbohydrazone is attributed to the ν(C=N) stretch, one of which undergoes a shift to lower frequency (1595–1602 cm^{-1}) in the spectra of molybdenum complexes designating the coordination of azomethine nitrogen to the metal centre.[7][,2(d)] This leads to the appearance of a new band at 620–640 cm^{-1} in the spectra of molybdenum complexes ascribed to the ν (Mo–N) stretch. The band appearing at 1386 cm^{-1} for the ligand matches to the stretching vibration of NH–C=S group and the consequent disappearance of this band in the spectra of the complexes signposts the tautomerisation of this functionality and the subsequent coordination of the thiol sulfur to the metal after its deprotonation. Moreover this gives rise to a new band in the spectra of the complexes in the range 1016–1027 cm^{-1} signalling the ν(C-S) stretching vibration. Whereas the bands at 1151 cm^{-1} and

1104–1190 cm^{-1} in the spectra of the ligand and the complexes respectively corresponds to the ν(N–N) vibration.

Finally the spectra of the molybdenum complexes exhibit two bands in the ranges 923–936 cm^{-1} and 896–906 cm^{-1} assigning to the symmetric and antisymmetric stretching vibrations[23] of the $[MoO_2]^{2+}$ core. The results of the FT-IR spectral assignments are provided in Table S1.

3.2.2 | Electronic spectra

The electronic spectra of the dithiocarbohydrazone, H_3TCL and its molybdenum complexes **1–3** were recorded in DMF at room temperature and using 1 x 10^{-5} M solution. The spectrum of dithiocarbohydrazone exhibits three absorptions at λ = 327, 346 and 363 nm assigned to π → π* and n → π* transitions of phenyl rings of the salicylaldehyde part and C=S moiety respectively.[7] The electronic spectra of the molybdenum complexes are almost similar proposing that they have principally similar structure. In addition to the bands corresponding to π → π* and n → π* transitions, they exhibit bands in the range 414–421 nm attributed to the charge transfer transition (LMCT) from the highest occupied molecular orbital of the dithiocarbohydrazone to the lowest unoccupied molecular orbital of the molybdenum ion.[6,7] The dearth of absorption in the visible region arising as a result of d-d transitions confirms the $4d^0$ electronic configuration of the central metal ion, Mo (VI).[6,7] The results of electronic spectral assignments of the synthesized compounds are given in Table S2.

3.2.3 | ^{1}H-NMR spectra

The ^{1}H-NMR spectra of the dithiocarbohydrazone and its molybdenum complexes were recorded in DMSO. The ^{1}H-NMR spectrum of the dithiocarbohydrazone, H_3TCL exhibits two $OH_{phenolic}$ protons at δ = 12.072 and 11.875 ppm, whereas the spectra of complexes adopt only one $OH_{phenolic}$ signal at 11.921 ppm since the other OH proton is involved in bonding with molybdenum ion. Although the ligand exhibits two NH signals at 11.618 and 9.142 ppm, the spectra of the complexes **1–3** display only one signal at 10.440, 10.484 and 10.443 ppm respectively due to the involvement of the other NH proton in the enolisation and deprotonation with subsequent coordination to molybdenum ion. Likewise the spectrum of the dithiocarbohydrazone displays two azomethine proton signals at 8.754 and 8.546 ppm, one of which undergoes downfield shift on coordination with molybdenum ion during complexation. The aromatic protons of both the dithiocarbohydrazone and its complexes were observed at the expected region of 6.811–8.284 ppm. The OCH_2 and CH_3 protons were observed in the region 4.055–4.073 ppm and 1.357–1.364 ppm respectively (Table S3). ^{1}H-NMR spectra of the dithiocarbohydrazone, H_3TCL and its molybdenum complexes are displayed Figures S1-S3.

3.3 | Electrochemical studies

The electrochemical studies of the dithiocarbohydrazone and its molybdenum complexes were evaluated by cyclic voltammetry in 10^{-5} M DMSO solution of the compounds. The results are summarized in Table 1.

The cyclic voltammograms of the dithiocarbohydrazone show irreversible oxidative and reductive peaks at 0.311 and − 0.510 V respectively. Both the complexes **1** and **3** **exhibited** irreversible reductive peak at −0.512 V which may be due to the redox behaviour of the dithiocarbohydrazone and do not account for the molybdenum centre. On the other hand, the irreversible reductive responses exhibited by the complexes **2** and **3** at −0.533 and − 0.294 V can be ascribed to the Mo (VI)/Mo(V) process.[24,6.7]

3.4 | Crystal structure description

3.4.1 | Collective features of the molybdenum complexes, 1–3

Diffraction quality single crystals of the complexes **1–3** obtained were subjected to single crystal X-ray diffraction analysis. The ORTEP plots of the complexes are displayed in Figure 4. Table S4 summarizes the crystal refinement details of the complexes and the important bond lengths and bond angles are collated in Table S5.

TABLE 1 Results of the cyclic voltammetric analysis of the dithiocarbohydrazone, H_3TCL and its molybdenum complexes **1–3**

Compound	E_{pc} [V][a]
H_3TCL	0.311, −0.510
Complex **1**	−0.512
Complex **2**	−0.533
Complex **3**	−0.294, −0.512

[a]Solvent: DMSO, Working electrode: Pt rod, Auxiliary electrode: Pt wire, Reference electrode: Ag/AgCl, Supporting electrolyte: 0.1 M TEAP, Scan rate: −100 mV/s. E_{pc} is the cathodic potential.

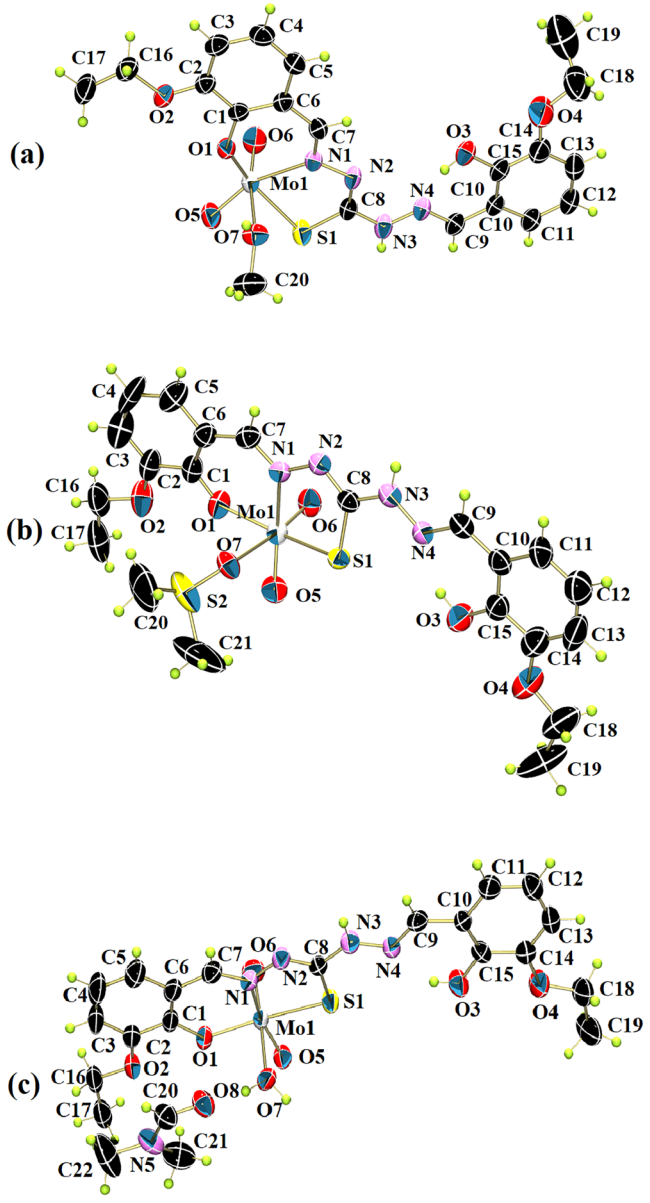

FIGURE 4 The ORTEP plots of complexes **1**–**3** (a-c) with atom numbering scheme for all non-hydrogen atoms. (Displacement ellipsoid drawn at 50% probability)

Complexes **1** and **3** got crystallized in monoclinic $P2_1/c$ space group whereas complex **2** in orthorhombic *P*bca space group. In complex **3**, a DMF molecule is present without coordination to the central metal, molybdenum. In all the complexes, the dithiocarbohydrazone ligand, H_3TCL performs as an ONS donor tridentate ligand despite being a potential pentadentate ligand. The molybdenum centre in all the three complexes portrays a distorted octahedral geometry where it coordinates with the three donor atoms of the ligand *viz.* the thioenolic sulfur, S(1); azomethine nitrogen, N(1) and phenolic oxygen, O(1). Further the molybdenum centre is coordinated by two oxido oxygen atoms, O(5) and O(6). Finally the oxygen atom, O(7) from the coordinated methanol molecule, DMSO molecule and H_2O molecule of the respective complexes **1**–**3** bond to the sixth coordination sphere of the complex accomplishing the expected prerequisite of molybdenum hexacoordination.[5–7]

Analogous to other reported *cis*-dioxidomolybdenum (VI) complexes, the molybdenum atom in all the three complexes are shifted from the centre of the octahedron by 0.2 Å towards the terminal oxido oxygen, O(4).[5–7] The two oxido oxygen atoms, O(4) and O(5) are*cis* positioned to each other and the Mo=O distances of the corresponding oxido oxygen atoms fall in the usual range of 1.693(2) and 1.689(2) Å for complex **1**; 1.680(4) and 1.702(4) Å for complex **2** and 1.709(2) and 1.670(3) Å for complex **3**. Likewise the Mo–S bond lengths for the complexes were also observed in the expected range of 2.4314 (9)-2.4393(10) Å. The Mo–N bond lengths for the complexes, 2.277(2) Å for complex **1**, 2.256(5) Å for complex **2** and 2.242(3) Å for complex **3** were observed to be rather long in consequence of the *trans* effect of the terminal oxido ligand, O(5). Regardless of this, all the other molybdenum-ligand bond lengths well fit with the bond length range for other reported *cis*-dioxidomolybdenum complexes.[6,7]

The *cis* bond angles observed for the complexes range from 81.92(9)-83.33(17) º for N(1)–Mo(1)–O(1), 76.17(7)-76.31(7)º for N(1)–Mo(1)–S(1), 87.91(8)-89.55(9) º for S (1)–Mo(1)–O(5) and 104.65(19)-107.32(11) º for O(1)–Mo (1)–O(5), whereas the *trans* angles range from 151.94(7)-154.25(12) º for O(1)–Mo(1)–S(1), 157.79(19)-159.65(11) º for N(1)–Mo(1)–O(5) and 168.42(11)-170.85(17) º for O (6)–Mo(1)–O(7). Incorporation of molybdenum into a five membered ring accounts for these distortions to a greater extent.

From the ring puckering analysis and least square plane calculations,[25] it is evident that the five membered chelate ring, Cg(1) comprising the Mo atom, Mo(1)/S(1)/C(8)/N(1)/N(2) in complexes **1**–**3** are puckered with puckering amplitudes of Q2 = 0.1442(19), 0.303(3) and 0.242(2) Å and ϕ = 11.0(11)°, 7.1(9)° and 197.1(9)° respectively. Similarly the six membered chelate ring, Cg (2) comprising the Mo atom, Mo(1)/O(1)/C(1)/C(6)/C(7)/N(2) of complex **1** is puckered with puckering amplitude Q2 = 0.260(2) Å and ϕ = 204.0(7)°.

3.4.2 | Supramolecular aspects

The supramolecular architectures of all the complexes were driven by several non-covalent interactions including hydrogen bonding, π···π and C–H···π interactions.

The crystal structure of complex **1** is stabilized by classical intra- and intermolecular hydrogen bonding

interactions. The phenolic proton, H(3′) and amino proton, (H3A) attached to the phenolic oxygen, O(3) and amino nitrogen, N(3) respectively are involved in intra and inter-molecular hydrogen bonding interaction with the azomethine nitrogen, N(4), O(3)–H(3′)···N(4) and oxido oxygen, O(6), N(3)–H(3A)···O(6) [x, 1/2-y, −1/2 + z] respectively (Figure S4).

In addition to that, the crystal structure is further stabilized by π···π and C–H···π interactions where the π cloud of the phenolic ring [C(1)/C(2)/C(3)/C(4)/C(5)/C(6)] bonded to molybdenum atom, Cg(3) of one molecule is involved in π···π interaction with the π cloud of the similar phenolic ring of the adjacent molecule with a centroid-centroid distance of 3.669(2) Å (Figure S4). Similarly a C–H···π interaction exist between the ethoxy proton, H(17B) of the phenolic ring coordinated to molybdenum with the π cloud of the phenolic ring that is not coordinated to the Mo centre, Cg(4) with a centroid-centroid distance of 3.756(5) Å (Figure S4).

Similarly complex **2** also exhibits the same two classical hydrogen bonding interactions exhibited by complex **1**, *viz.* O(3)–H(3′)···N(4) and N(3)–H(3A)···O(5) [1/2 + x, y, −1/2-z]. In addition to that the crystal structure consists of two more non-classical intermolecular hydrogen bonding interactions where the ethoxy proton of the phenolic ring that is not coordinated to the Mo centre is coordinated with the oxido oxygen atom, O(6) of the adjacent molecule, C(19)–H(19C)···O(6), [2-x, 1-y, 1-z] and the methoxy proton of the coordinated DMSO molecule, H(21B) is hydrogen bonded to the phenolic oxygen atom, O(3) of the adjacent molecule, C(21)–H(21B)···O(3), [1-x, 1-y, 1-z] (Figure S5).

Complex **3** exhibits two classical hydrogen bonding interactions similar to complexes **1** and **2** where the phenolic proton, H(3A) attached to the phenolic oxygen, O(3) is involved in intramolecular hydrogen bonding interaction with the azomethine nitrogen, N(4), O(3)–H(3A)···N(4). Unlike complexes **1** and **2**, the amino proton, (H3N) is involved in intermolecular hydrogen bonding interaction with the oxygen atom, O(8) of the uncoordinated DMF molecule, N(3)–H(3 N)···O(8) [1-x, 1-y, 1-z] rather than the oxygen atom, O(7) of the coordinated water molecule. The methoxy protons, H(21B) and H(21C) of the uncoordinated DMF molecule are engaged in intra- and intermolecular hydrogen bonding interaction with ethoxy oxygen atom, O(2), C(21)–H(21B)···O(2) and phenoxy oxygen atom, O(3), C(21)–H(21B)···O(3) [1-x, 1-y, 1-z] respectively (Figure S6).

Crystal structure of complexes **2** and 3 do not exhibit any π–π or C–H···π interactions. The interaction parameters for the various hydrogen bonding, π–π and C–H···π interactions present in the crystal structures of the molybdenum complexes are summarized in Tables S6, S7 and S8 respectively.

3.5 | Hirshfeld surface analysis

The visualization and quantification of the close contacts present in the crystal structures of all the three complexes were assured with the aid of Crystal Explorer 17.5 software. The Hirshfeld surface and the associated fingerprint plots of the complexes were computed.

Figure 5 portrays the Hirshfeld surfaces of the complexes **1**–**3** mapped over d_{norm}, shape index and curvedness. The d_{norm} surfaces (ranged between −0.5871 to 1.3351 Å for complex **1**, −0.4479 to 1.5473 Å for complex **2** and − 0.5963 to 1.5387 Å for complex **3**) are transparently shown to visualize the moieties around which it was calculated. The bright red spots present in the d_{norm} surface[25] signifies the hydrogen bond centres, whereas the pale coloured regions signpost the weak and long range intermolecular interactions. Similarly the red spots in shape index indicate the hydrogen bonding interactions and the complimentary hydrogen bonding interactions are displayed as blue spots. In addition to that the π–π and C–H···π interactions appear as 'bow-tie' patterns in the shape index plot,[26] however these interactions appear as flat regions in the curvedness plot.

The two dimensional fingerprint plots displayed in the range 1.0–2.4 Å with the d_e (the closest external) and d_i (the closest internal) distance scales displayed on graph axes showcases particular atom-pair contacts and aids the parting of contributions from different interaction types that overlap in the full fingerprint plot.[26,27] The fingerprint plots of the complexes are provided in Figure S7.

H···H interactions are the most recurrent interactions in the complexes encompassing about 44, 47.4 and 43.5% of the total Hirshfeld surface of the complexes **1**, **2**and 3 respectively ascribed to the abundance of hydrogen on the molecular surface. These interactions appear as two end points that points towards the origin. Whereas the second largest interaction is the O···H interaction which appear as two distinct spikes of almost equal length in the 2D fingerprint plots contributing to 22, 25 and 29.4% of the total Hirshfeld surface of the complexes **1**, **2** and **3** respectively. Similarly the C···H interactions appear as two symmetrical wings on left and right side and corresponds to 14, 11.4 and 13.2% of the total Hirshfeld surface of the complexes **1**, **2** and **3** respectively. Other weak interactions like S···H (4.1, 4.5 and 4.2% of the total Hirshfeld surface for complexes **1**, **2** and **3** respectively), N···H (5.7, 3.1 and 3.9% of the total Hirshfeld surface for complexes **1**, **2** and **3** respectively) and C···C (3.5% for complex **1**) are characterized by their small space

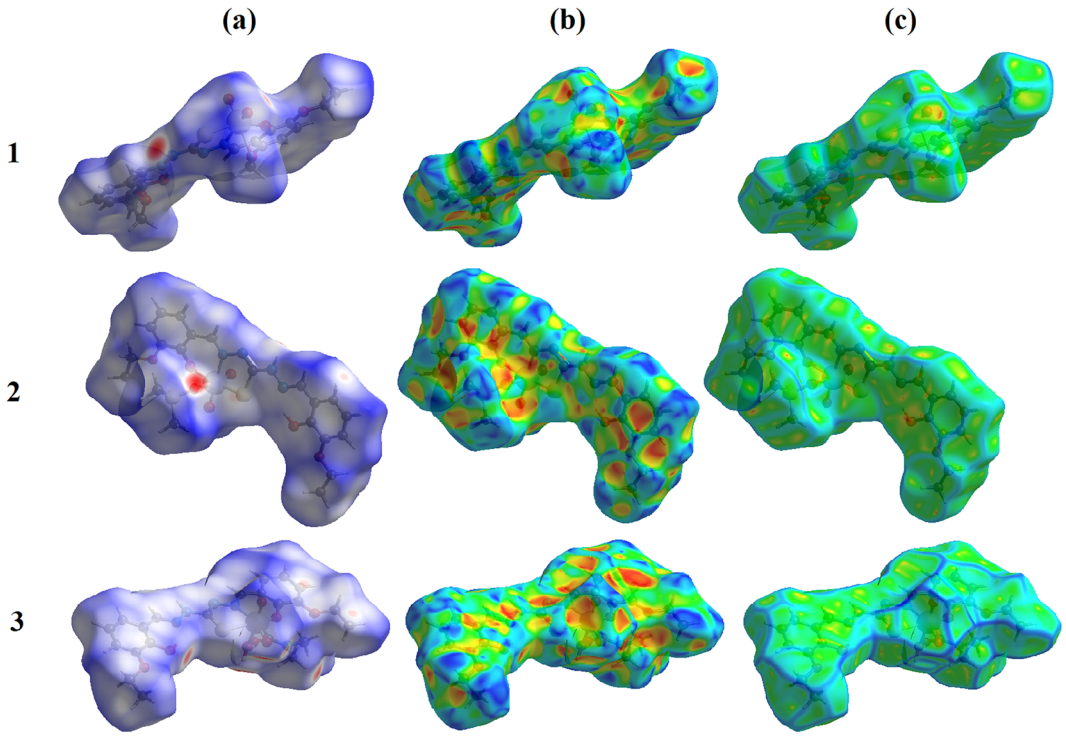

FIGURE 5 Hirshfeld surface of complexes **1–3** mapped with (a) d_{norm}, (b) shape index and (c) curvedness

occupations in the fingerprint plot. Relative contributions from all major interactions to the Hirshfeld surface are detailed in Figure 6.

Hirshfeld surface analysis also assists in envisioning the prominent hydrogen bonding interactions present in the complexes. Important hydrogen bonding interactions of complex **1** are portrayed in Figure S8.

3.6 | Antioxidant activity studies

The antioxidant activity of the dithiocarbohydrazone, H_3TSL and its molybdenum complexes were evaluated by DPPH, ABTS and total antioxidant assays with respect to the standard antioxidant, *L* ascorbic acid.

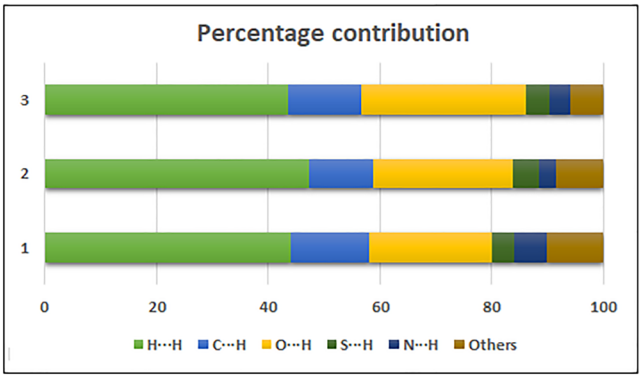

FIGURE 6 Percentage contributions to the Hirshfeld surface area for the various close intermolecular contacts for molecules **1–3**

In the DPPH assay the dithiocarbohydrazone, H_3TCL and its molybdenum complexes displayed good antioxidant capacity by reducing the stable violet coloured DPPH radical to the yellow coloured diphenyl picryl hydrazine.

The radical scavenging activities of the compounds were studied at different concentrations (10–100 μM) of the compounds under study and the activity followed a dose dependent manner. The results of the analysis was then expressed as their IC_{50} values (Figure 7). The molybdenum complexes exhibited lower IC_{50} values and higher activity compared to the dithiocarbohydrazone ligand. The standard, *L*-ascorbic acid failed to produce 50% inhibition at the studied concentration range. Therefore the DPPH radical scavenging ability of the compounds followed the order Ascorbic acid< H_3TCL < Complex **1** < Complex **3** < Complex **2**. The expected mechanism for the DPPH assay of these compounds are exhibited in Scheme 3.

A possible mechanism for the antioxidant activity of the synthesized compounds are being discussed in Scheme 3 by considering dithiocarbohydrazone as the representative example. Generally the antioxidant activity of a compound depends on the number of hydrogen atoms available for donation to the DPPH radical. In the case of the dithiocarbohydrazone, the acidic hydrogen (responsible for thioketo-thioenol tautomerism in

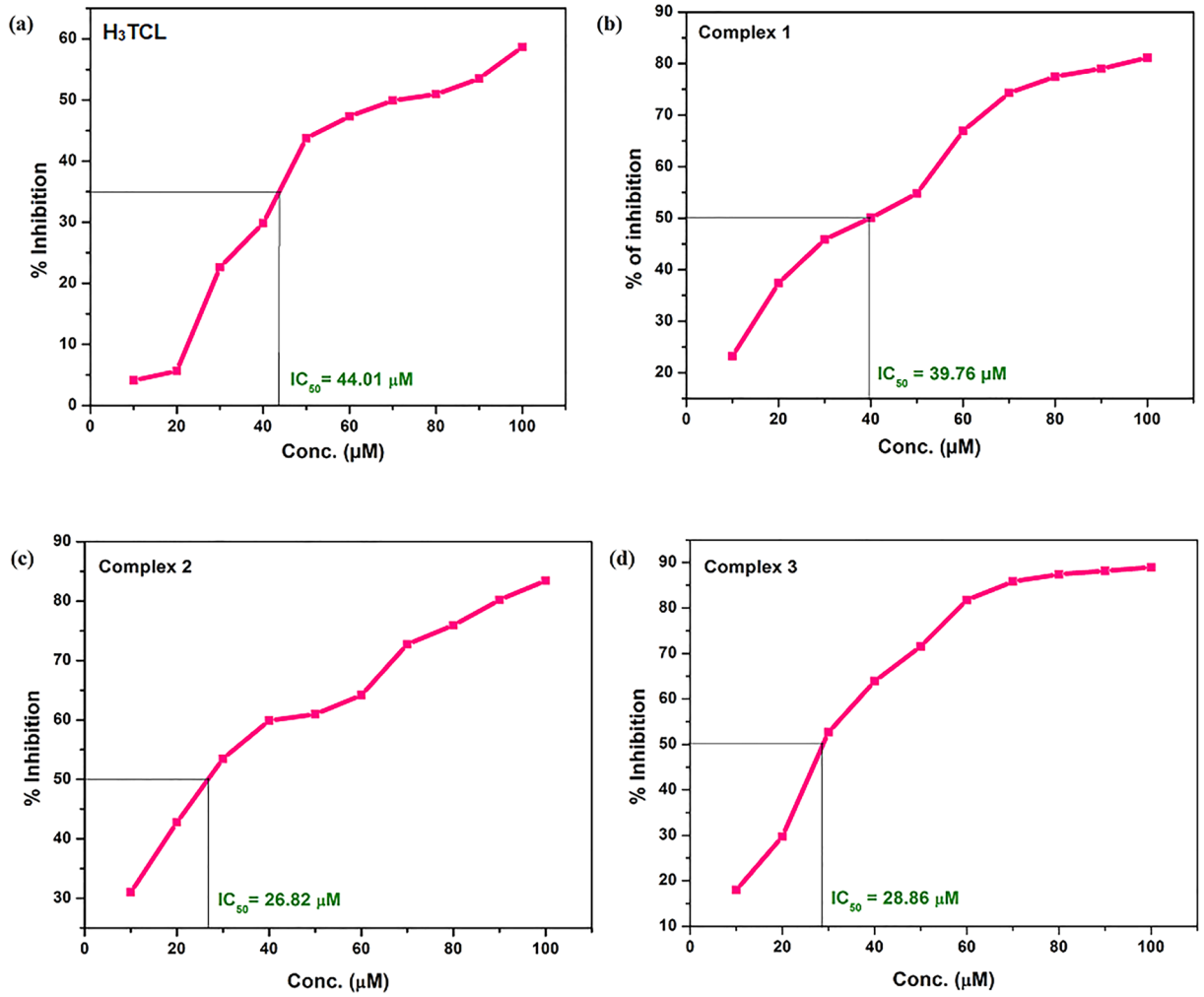

FIGURE 7 The results of DPPH antioxidant assay of the dithiocarbohydrazone and its molybdenum complexes

H_3TCL) shown in red colour stabilises the DPPH radical resulting in the formation of a new radical (radical A) which is resonance stabilized. But when it comes to the case of molybdenum complexes, the acidity of the hydrogen involved in the scavenging of DPPH radical increases due to the electron withdrawing effect of the metal, molybdenum which exist in its highest possible oxidation state (+6), thereby increasing the radical scavenging ability of the resultant complexes. Moreover the uncoordinated phenolic proton can also contribute to the antioxidant activity. But the role of coordinated solvent molecules towards antioxidant activity is still unknown.

The radical scavenging ability of the tested compounds towards the ABTS radical cation characteristically showed that even though the tested compounds were less efficient antioxidants compared to the standard antioxidant, *L*-ascorbic acid, the molybdenum complexes displayed higher activity compared to the free dithiocarbohydrzone, H_3TCL (Figure 8(a)). The activity followed the order *L*-ascorbic acid> complex **3** > complex **1** > complex **2** > H_3TCL.

The total antioxidant capacity of the dithiocarbohydrazone and its molybdenum complexes evaluated by the phosphor-molybdenum method also showed that these compounds exhibit antioxidant activities comparable to that of the standard antioxidant, *L*-ascorbic acid (Figure 8(b)). Among the tested compounds, complex **1** exhibited the maximum AEAC (Ascorbic acid equivalent antioxidant capacity). The activity followed the order, Complex **2** < H_3TCL < Complex **3** < Complex **1**.

Table 2 summarises the results of the various antioxidant assays.

To conclude, the dithiocarbohydrazone and its molybdenum complexes displayed good antioxidant capacities where the former exhibited much lesser activity compared to the latter which can be attributed to the chelation of the ligand with the molybdenyl cation.

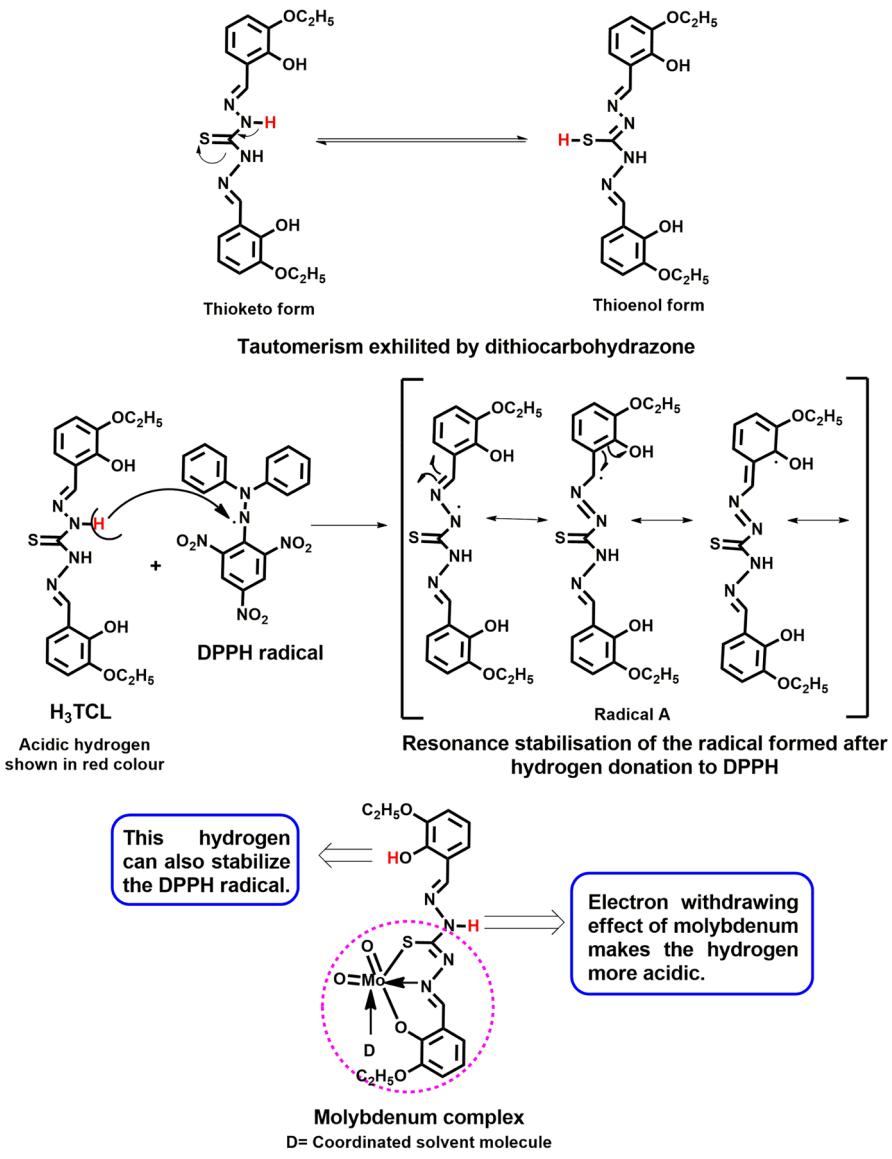

SCHEME 3 Possible mechanism of DPPH radical scavenging by the thiocarbohydrazone ligand and its molybdenum complexes

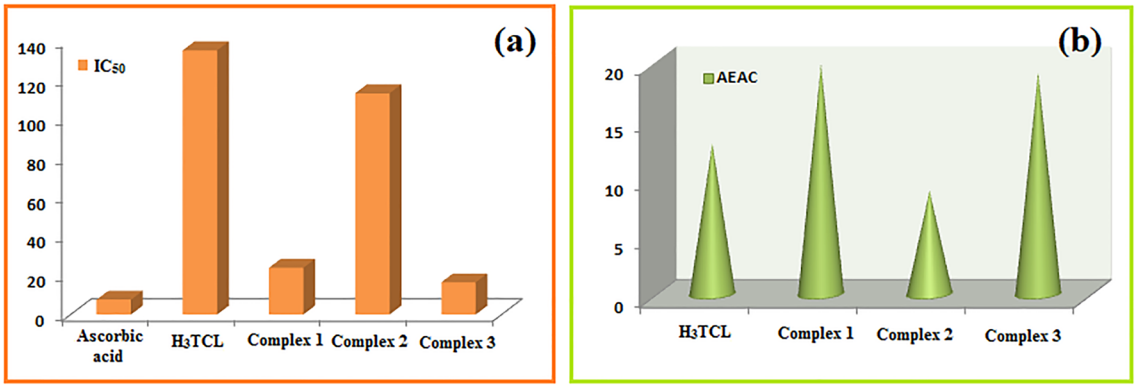

FIGURE 8 The results of (a) ABTS antioxidant assay and (b) total antioxidant assay of the dithiocarbohydrazone and its molybdenum complexes

TABLE 2 Results of various antioxidant assays

Compound	DPPH antioxidant assay (IC_{50} values (μM))	ABTS antioxidant assay (IC_{50} values (μL))	Total antioxidant assay (AEAC)[a] (μg)
H_3TCL	44.01	135	12.91
Complex **1**	39.76	23.91	19.17
Complex **2**	26.82	113	8.86
Complex **3**	28.86	16.49	19.04
L-ascorbic acid	-	7.58	-

[a]Ascorbic acid equivalent antioxidant capacity = antioxidant capacity of the compound equivalent to that of 1 g ascorbic acid.

4 | CONCLUSION

In the present work, we have included studies on a new dithiocarbohydrazone and its three molybdenum complexes. These complexes exhibit a 1:1 metal ligand stoichiometry from the analytical data. All complexes were found to be non-electrolytes in DMF solution and exhibited an irreversible redox behaviour as revealed by the cyclic voltammetric studies. The spectral characterisation along with the single crystal X-ray diffraction analysis revealed that the dithiocarbohydrazone binds with Mo ion in a tridentate fashion through nitrogen atom of the azomethine and oxygen atoms of hydroxyl group of the 3-ethoxysalicylaldehyde besides the thioenolate sulfur from the dithiocarbohydrazide moiety in all the complexes. The evaluation of antioxidant activities of the dithiocarbohydrazone and its complexes by various antioxidant assays disclosed that the metal complexes exhibited higher free radical scavenging abilities compared to the free dithiocarbohydrazone ligand. The Mo complexes are capable of donating electron or hydrogen atom and subsequently react with free radicals or terminate chain reactions in a dose-dependent pattern. Further these observations were validated with the aid of molecular docking approaches (provided in the supplementary information, Figure S9 and Table S9) which revealed that the antioxidant activity exhibited by the compounds are directly dependent on the extend of interaction of them with the amino acid residues present in the active site of the human antioxidant enzyme, 3MNG. Greater the number of conventional hydrogen bonding interactions between the two, greater will be the binding constant value and hence greater will be the antioxidant activity.

ACKNOWLEDGMENTS

T.M. Asha acknowledges the Council for Scientific and Industrial Research (CSIR), New Delhi, India for the award of a Senior Research Fellowship (09/239(0510)/2015-EMR-I). The authors are thankful to the Sophisticated Analytical Instrumentation Facility, Cochin University of Science and Technology, Kochi, India for elemental analysis & single crystal X-ray diffraction measurements and Octagon Scientific Services Private Ltd., Tiruchirapally, Tamil Nadu, India for ^{1}H NMR spectral analysis.

APPENDIX A. SUPPLEMENTARY DATA

CCDC 1972016, 1972017 and 1972018 contain the supplementary crystallographic data for complexes **1**, **2** and **3** respectively. These data can be obtained free of charge *via*www.ccdc.cam.ac.uk/conts/retrieving.html or from the Cambridge Crystallographic Data Centre, 12 Union Road, Cambridge CB2 IEZ, UK; fax: (+44) 1223–336-033; or e-mail: deposit@ccdc.cam.ac.uk.

ORCID

M.R. Prathapachandra Kurup https://orcid.org/0000-0002-9434-890X

REFERENCES

[1] (a) S. L. A. Kumar, M. S. Kumar, S. J. Jenniefer, P. T. Muthiah, A. Sreekanth, *Phosphorus, Sulfur Silicon Relat. Elem.* **2013**, *188*, 1110. (b) R. Bikas, R. Karimian, M. Siczek, S. Demeshko, H. Hosseini-Monfared, T. Lis, *Inorg. Chem. Commun.* **2016**, *70*, 219.

[2] (a) M. T. Gabr, N. S. El-Gohary, E. R. El-Bendary, M. M. El-Kerdawy, N. Ni, *Eur. J. Med. Chem.* **2017**, *128*, 36. (b) C. Bonaccorso, G. Grasso, N. Musso, V. Barresi, D. F. Condorelli, D. L. Mendola, E. Rizzarelli, *J. Inorg. Biochem.* **2018**, *182*, 92. (c) A. A. A. Abou-Husseina, W. Linert, *Spectrochim. Acta Part a: Mol. And Biomol. Spectr.* **2012**, *95*, 596. (d) E. Manoj, M. R. P. Kurup, A. Punnoose, *Spectrochim. Acta Part a: Mol. And Biomol. Spectr.* **2009**, *72*, 474. (e) D. N. A. Chee, M. Affan, F. B. Ahmad, M. Asaruddin, N. Sam, M. A. Salam, A. Ismail, S. H. Tan, *J. Coord. Chem.* **2011**, *64*, 4191.

[3] (a) H. Gang, G. Dong, D. Chun-Ying, M. Hong, M. Qing-jin, *New J. Chem.* **2002**, *26*, 1371. (b) M. A. Ali, P. V. Bernhardt, C. L. Kiem, A. H. Mirza, *Aust. J. Chem.* **2004**, *57*, 409. (c) H. Cheng, D. Chun-ying, F. Chen-jie, L. Yong-jiang, M. Qingjin, *J. Chem. Soc. Dalton Trans.* **2000**, 1207. (d) E. Manoj, M. R. P. Kurup, R. P. John, M. Nethaji, A. Punnoose, *Inorg. Chem. Commun.* **2009**, *12*, 952. (e) E. Manoj, M. R. P. Kurup, H. -K. Fun, A. Punnoose, *Polyhedron* **2007**, *26*, 4451.

[4] I. Bertini, *Biological Inorganic Chemistry: Structure and Reactivity*, University Science Books, Sausalito, California **2007**.

[5] (a) M. R. Maurya, L. Rana, N. Jangra, F. Avecilla, *ChemSelect* **2017**, *23*, 6767. (b) A. Bezaatpour, E. Askarizadeh, S. Akbarpour, M. Amiria, B. Babaei, *Mol. Catal.* **2017**, *436*, 199. (c) E. B. Seena, M. R. P. Kurup, *Polyhedron* **2007**, *26*, 3595. (d) A. A. Aravindakshan, B. Joseph, U. L. Kala, M.R. P. Kurup, *Polyhedron* **2017**, *123*, 206. (e) T. M. Asha, M. R. P. Kurup, *J. Chem. Crystallog.* **2019**, *49*, 219. (f)

D. Biswal,N. R. Pramanik, S. Chakrabarti, M. G. B. Drew, *Inorg. Chim. Acta* **2016**, *451*, 92. (g) T. M. Asha, M. R. P. Kurup, *J. Mol. Struct.* **2020**, *1204*, 127553. (h) T. M. Asha, E. Shiju, C. Keloth, M. R. P. Kurup, *Appl. Organomet. Chem.* **2020**, *34*, e5520. https://doi.org/10.1002/aoc.5520

[6] (a) T. M. Asha, M. R. P. Kurup, *Inorg. Chim. Acta* **2018**, *483*, 44. (b) T. M. Asha, M. R. P. Kurup, *Polyhedron* **2019**, *169*, 151. (c) S. Pasayat, S. P. Dash, Saswati, P. K. Majhi, Y. P. Patil, M. Nethaji, H. R. Dash, S. Das, R. Dinda, *Polyhderon* **2012**, *38*, 198. (d) J. Pisk, L. Bilić, M. Đaković, D. Cvijanović, V. Damjanović, J. Lovrić, M. Rubčić, V. Vrdoljak, M. Cindric, *Polyhedron* **2018**, *145*, 70.

[7] (a) T. M. Asha, M. Sithambaresan, M. R. P. Kurup, *Polyhedron* **2019**, *171*, 530. (b) M. A. Hussein, T. S. Guan, R. A. Haque, M. B. K. Ahamed, A. M. S. A. Majid, *Inorg. Chim. Acta* **2014**, *421*, 270. (c) M. A. Hussein, T. S. Guan, R. A. Haque, M.B. K. Ahamed, A. M. S. A. Majid, *Polyhedron* **2015**, *85*, 93.

[8] R. Scherer, H. T. Godoy, *Food Chem.* **2009**, *112*, 654.

[9] S. K. Kurapati, S. Pal, *Appl. Organomet. Chem.* **2016**, *30*, 116.

[10] S. Y. Ebrahimipour, M. Khosravan, J. White, S. Fekri, *Appl. Organomet. Chem.* **2018**, *32*, e4233.

[11] (a) D. Biswal, N. R. Pramanik, S. Chakrabarti, M. G. B. Drew, P. Mitra, K. Acharya, S. Biswase, T. K. Mondale, *New J. Chem.* **2015**, *39*, 8681. (b) S. Eğlence, M. Şahin, M. Özyürek, R. Apak, B. Ülküseven, *Inorg. Chim. Acta* **2018**, *469*, 495. (c) A. A. Shanty, P. V. Mohanan, *Spectrochim. Acta Part a: Mol. And Biomol. Spectr.* **2018**, *195*, 181.

[12] SMART and SAINT, Area Detector Software Package and SAX Area Detector Integration Program, Bruker Analytical X-ray, Madison, WI, USA, **1997**.

[13] SADABS, *Area Detector Absorption Correction Program*, Bruker Analytical X-ray Madison, WI, USA **1997**.

[14] G. M. Sheldrick, *Acta Crystallogr. C* **2015**, *71*, 3.

[15] L. J. Farrugia, *J. Appl. Cryst.* **2012**, *45*, 849.

[16] K. Brandenburg, Diamond version 3.2g, Crystal Impact GbRBonn, Germany, **2011**.

[17] M. J. Turner, J. J. McKinnon, S. K. Wolff, D. J. Grimwood, P. R. Spackman, D. Jayatilaka, M. A. Spackman, CrystalExplorer17, University of Western Australia, **2017**.

[18] (a) J. J. McKinnon, D. Jayatilaka, M. A. Spackman, *Chem. Commun.* **2007**, 3814. (b) M. A. Spackman, J. J. McKinnon, *CrstEngComm* **2002**, *4*, 378.

[19] W. Brand-Williams, M. E. Cuvelier, C. Berset, *LWT- Food Sci. Technol.* **1995**, *28*, 25.

[20] (a) Y. X. Zhao, J. Dou, T. Wu, A. Haji, *Molecules* **2013**, *18*, 951. (b) V. Roginsky, E. A. Lissi, *Food Chem.* **2005**, *92*, 235.

[21] C. I. G. Tuberoso, M. Boban, E. Bifulco, D. Budimir, F. M. Pirisi, *Food Chem.* **2013**, *140*, 686.

[22] P. Prieto, M. Pineda, M. Aguilar, *Anal. Biochem.* **1999**, *269*, 337.

[23] A. Peuronen, R. Sillanpää, A. Lehtonen, *Chem. Select* **2018**, *3*, 3814.

[24] (a) S. Purohit, A. P. Koley, L. S. Prasad, P. T. Manoharan, S. Ghosh, *Inorg. Chem.* **1989**, *28*, 3735. (b) I. W. Boyd, J. T. Spence, *Inorg. Chem.* **1982**, *21*, 1602. (c) B. B. Kaul, J. H. Enemark, S. L. Merbs, J. T. Spence, *J. Am. Chem. Soc.* **1985**, *107*, 2885.

[25] D. Cremer, J. A. Pople, *J. Am. Chem. Soc.* **1975**, *97*, 1354.

[26] J. J. McKinnon, D. Jayatilaka, M. A. Spackman, *Chem. Commun.* **2007**, *n/a*, 3814.

[27] (a) S. S. Sreejith, A. Nair, V. A. Smolenski, J. P. Jasinski, M.R. P. Kurup, *Inorg. Chim. Acta* **2018**, *469*, 264. (b) S.S. Sreejith, N. Mohan, M. R. P. Kurup, *Polyhedron* **2017**, *1145*, 170.

SUPPORTING INFORMATION

Additional supporting information may be found online in the Supporting Information section at the end of this article.

How to cite this article: Asha TM, Prathapachandra Kurup MR. An insight into the potent antioxidant activity of a dithiocarbohydrazone appended *cis*-dioxidomolybdenum (VI) complexes. *Appl Organomet Chem*. 2020;e5762. https://doi.org/10.1002/aoc.5762